

Preparation and in Vitro Degradation Behavior of Mg-based Foam Biomaterials for Bone Tissue Engineering

Huang Wenzhan, Luo Hongjie, Mu Yongliang, Xu Jianrong

Engineering Research Center of Ministry of Education for Advanced Materials Preparation Technology, Northeastern University, Shenyang 110819, China

Abstract: Mg-based foam biomaterials were prepared by a melt foaming process, with Mg-Ca alloy as the matrix material, hydroxyapatite (HA) as the tackifier, and MgCO₃ as the foaming agent. The Mg-based foam biomaterials with uniform structure were tested to investigate their biodegradable behaviors. The biodegradable property of the Mg-based foam was mainly characterized by microstructure observations, immersion tests and electrochemical measurements. The results show that the weight loss rate increases with increasing the porosity of the specimen within a fixed period of time. The weight loss rate of the specimen without HA particles is much higher than that of the specimen with HA particles. Meanwhile, the open porosity of the Mg-based foam biomaterial increases with immersion time. Both the total porosity and added HA content have an important effect on the open porosity of the Mg-based foam biomaterial. Within a fixed period of time, the open porosity of the Mg-based foam biomaterial increases with the increase of the total porosity. Mg-based foam biomaterials added with HA exhibit higher corrosion resistance than Mg-based foam biomaterials without HA in simulated body fluid (SBF) media.

Key words: Mg-based foams; biomaterials; biodegradable behavior; immersion test; electrochemical measurement; HA particles

Bone substitutes are often required to replace damaged tissue caused by accidents, disease, trauma, or other types of damage. Therefore, designing appropriate scaffolds has received increasing attention from both an academic and industrial point of view, and it is one of the main challenges in tissue engineering (TE)^[1-4]. Currently, biomaterials for tissue engineering mostly consist of ceramics, polymers, hydrogels and metals^[3-8]. In the case of ceramics, polymers and hydrogels, the weakness in mechanical strength is the main concern for the applicability of the produced scaffolds, especially for bone TE. Metals are the most appropriate materials used for bone tissue engineering considering their unique mechanical strength as biomedical scaffolds and implants^[8,9]. Traditionally, Ti alloys and stainless steel have played an important role in repairing damaged bone tissues as biomedical metal implant materials. However, the main problem is that when metal implants exist in the human body for a long time, they may cause permanent physical irritation, and chronic

inflammatory discomfort, or release toxic elements that impair healthy^[10]. Biodegradable materials can avoid these problems by gradually being dissolved, absorbed, consumed, or excreted after the bone tissue has been healed.

Among biodegradable metals, Mg alloys are a new class of degradable biomaterials. Mg alloys with low densities have similar bioactivity and biodegradation properties to bone and promote bone growth^[11,12]. Three-dimensional (3D) porous Mg alloy scaffolds have potential for bone tissue engineering application due to their good mechanical properties and porous structure similar to that of natural bone. The three dimensional (3D) porous structures offer opportunities for the invasion, attachment and proliferation of cells and the formation of blood vessels. Meanwhile, implants can eventually be replaced by newly formed bone after the gradual degradation and absorption of the Mg alloy scaffolds^[12]. Porous Mg alloy scaffolds with different preparation methods can serve as implant biomaterials for bone tissue engineering

Received date: October 19, 2018

Foundation item: National Natural Science Foundation of China (51874093, 51174060, 51301109)

Corresponding author: Luo Hongjie, Ph. D., Professor, Engineering Research Center of Ministry of Education for Advanced Materials Preparation Technology, School of Metallurgy, Northeastern University, Shenyang 110819, P. R. China, Tel: 0086-24-83686462, E-mail: neuhjluo@sina.com

Copyright © 2019, Northwest Institute for Nonferrous Metal Research. Published by Science Press. All rights reserved.

applications^[12-15]. However, limited work has been done on the melt-foaming method to prepare the appropriate Mg alloy foams for use as biomaterials. The melt-foaming method is a simple technique for the preparation of metallic foams, and the preparation cost is low; therefore, it is promising for large-scale industrial production. As such, it is worthwhile to explore the biomedical application of Mg alloy foam prepared by the melt-foaming method.

In this paper, Mg-based foam biomaterials were fabricated by the melt-foaming method. The microstructure was observed and the total porosity and open porosity of the Mg-based foam biomaterials were tested. Immersion tests and electro-chemical measurements were performed to evaluate the degradation behavior of the Mg-based foam biomaterials. The effect of HA content and total porosity of the Mg-based foam biomaterials on the biodegradable behaviors was studied.

1 Experiment

1.1 Fabrication of Mg-based foam biomaterials

The raw material, Mg-3Ca alloy, was prepared by adding appropriate amounts of Mg to the Mg-20Ca matrix alloy at 700 °C. For the production of Mg-3Ca alloy, the matrix alloy was purchased from Shanxi Yinguang Magnesium Industry Group Co., Ltd. Closed-cell Mg-based foam biomaterials were fabricated by the melt foaming process. The process mainly focused on the following steps: (1) Mg-3Ca alloy was melted at 700°C in a stainless steel crucible heated by an electric resistance furnace. (2) The hydroxyapatite (HA) particles (0, 4, 6, 8, wt%, 100 μm in particle size) used as a thickening agent were added into the melt at 640 °C at a stirring speed of 1200 r/min for 300 s. (3) The MgCO₃ (120 μm) foaming agent was added to the melt at 610 °C by stirring, with the stirring speed of 1900 r/min for 180 s. (4) After being held in the furnace at 640 °C for 120 s, the crucible was removed and cooled to room temperature. The Mg-based foam biomaterials with total porosities in the range from 19.81% to 89.1% and a cell size in the range from 0.8 mm to 1.5 mm were obtained by altering the amount of foaming agent addition. Argon gas was applied to protect the melt from ignition or oxidation during the procedures.

1.2 Structure characterization

The Mg-based foam biomaterials were cut into 10 mm×10 mm×10 mm cubes by an electric discharge machine. The specimen's density was determined through its weight and physical dimensions, and the total porosity of the foam is defined as^[16]:

$$P_t = 1 - \frac{\rho}{\rho_s} \quad (1)$$

where P_t is the total porosity of the Mg-based foam biomaterial, and ρ and ρ_s are the densities of the Mg-based foam biomaterials and the cell wall material, respectively. In addition, morphological defects such as fractured or missed cell walls in Mg-based foam biomaterials make the closed cell

become interconnected; closed porosity will turn into open porosity. The open porosity of the Mg-based foam biomaterials was measured using vacuum water seepage. Under vacuum, the specimen was immersed in water for 2 h, during which the interconnected cell would be completely filled with water. Open porosity, a parameter describing cell connectivity, is calculated as follows:

$$P_o = \frac{V_w}{V_f} = \frac{M_w \rho}{M_f \rho_w} \quad (2)$$

where P_o is open porosity of the Mg-based foam biomaterials, V_w and V_f are the volume of water in the cells and the Mg-based foam biomaterials, respectively, M_w and M_f are the weight of water in the cells and the Mg-based foam biomaterials, respectively, and ρ_w is the density of water.

The microstructure of the sample was observed by a scanning electron microscope (SEM; Ultra Plus, Zeiss, Germany) equipped with an energy dispersive spectrometer (EDS; X-Max, Oxford Instruments, England). Phase analysis was performed by an X-ray diffractometer (XRD; X'Pert Pro, PANalytical B.V., Netherlands) operated with Cu K α ($\lambda=0.154\ 056\ \text{nm}$) radiation.

1.3 Immersion test

The size of the specimens for immersion test was 10 mm×10 mm×10 mm. Immersion tests were carried out in simulated body fluid (SBF) media at human body temperature (37±0.5 °C) using a water bath. During the immersion tests, the solution was changed every 72 h.

In different immersion periods, the biodegradation products were manually extracted using tweezers. The phase analysis of the biodegradation products was performed by X-ray diffractometer. Then, the specimens were rinsed in chromic acid solution (180 g/L) by ultrasonic cleaning in order to clean the biodegradation products on the surface before morphology observation. The degradation products react with chromic acid and dissolve in the solution without influencing the Mg substrate^[13, 17]. An certain amount of weight loss was detected before immersion in SBF media and after chromic acid immersion. The weight loss rate describing the specimen's loss rate in the immersion test is determined by:

$$W_r = (M_b - M_a) / M_b \quad (3)$$

where W_r is weight loss rate, and M_b and M_a are the weight of the specimen before immersion in SBF and after chromic acid immersion, respectively. In addition, the open porosity after the immersion test was also measured.

1.4 Electrochemical measurement

The electrochemical tests were carried out in SBF solution at 37±0.5 °C using an electrochemical workstation (CS350, Wuhan Corrtest Instruments Co., Ltd, Wuhan, China). The electrochemical properties were measured using a typical three electrode configuration: Mg-based foam biomaterials were the working electrode, the reference electrode was a saturated calomel electrode (SCE), and the counter electrode was a graphite rod. The specimen size for the electrochemical

test was 10 mm×10 mm×10 mm, and the testing area was 100 mm². A copper wire lead was attached to one side of each sample by close sealing with epoxy resin, leaving one end surface (with a cross-sectional area of 100 mm²) exposed to the SBF solution. The potentiodynamic polarization tests were carried out in 500 mL SBF solution at a scanning rate of 50 mV/s.

2 Results and Discussion

2.1 Morphology observation and phase composition of the Mg-based foam biomaterials

Fig.1 shows the SEM images of Mg-based foam biomaterial. The typical cell structure of the Mg-based foam biomaterials is shown in Fig.1a~1e. It can be seen that the cells are mostly closed-cell and irregular ellipses. Meanwhile, the Mg-based foam biomaterial exhibits uniform cell distribution with a size of 0.8~1.5 mm. Heterogeneities and morphological defects, such as fractured or missed cell walls and cell wall buckling, can be seen in the images, which may considerably affect the corrosion resistance. These defects create a certain number of interconnected cells in the closed-cell Mg foam, which results in easier penetration of the SBF liquid. Fig.1f shows the microstructure of cell edge in the Mg-based foam biomaterial. Spherical solid blocks (D) and some defects are distributed on the cell edge. It is confirmed by the EDS analysis that the spherical solid blocks (D) are HA particles that were added during melt foaming. It can be found that the HA particles are uniformly distributed in the cell wall of Mg-based foam biomaterial. At the same time, the interface between HA and

Mg alloy matrix can be observed distinctly.

The X-ray diffraction (XRD) pattern of the Mg alloy matrix reinforced by HA is shown in Fig.2. It can be found that the composite matrix is mainly composed of α -Mg, Mg₂Ca and HA. Ca is one of the common alloying elements in Mg and plays a crucial role in the formation of bone^[18, 19]. Previous studies have shown that Mg-Ca alloys degrade within bones and have good biocompatibility in vivo and in vitro^[20, 21]. Hydroxyapatite (HA) is currently used as a biomedical material and exhibits excellent biocompatibility and bioactivity due to its chemical and structural similarity to bone and tooth minerals^[10]. Therefore, it is concluded that Mg-based foam biomaterials are biocompatible, have appropriate biodegradation properties and will not release toxic elements impairing the health of the human body.

2.2 Immersion test

Fig.3a shows the change of weight loss rate of the specimens with different total porosities during the immersion period. It can be seen that the weight loss rate increases with the increase in immersion time. Two sets of specimens with high total porosity have higher weight loss rates than other specimens with low total porosity. It is clear that the weight loss rate increases with the increase in total porosities. This means that under the same immersion corrosion conditions, the higher the total porosity of the specimen, the higher the weight loss rate. After 14 d of immersion, it is shown that the weight loss rates of the specimens are 85.17%, 69.98%, 33.12% and 30.94% when the total porosity is 75.29%, 72.06%, 47.24% and 38.90%, respectively. Temporally, the

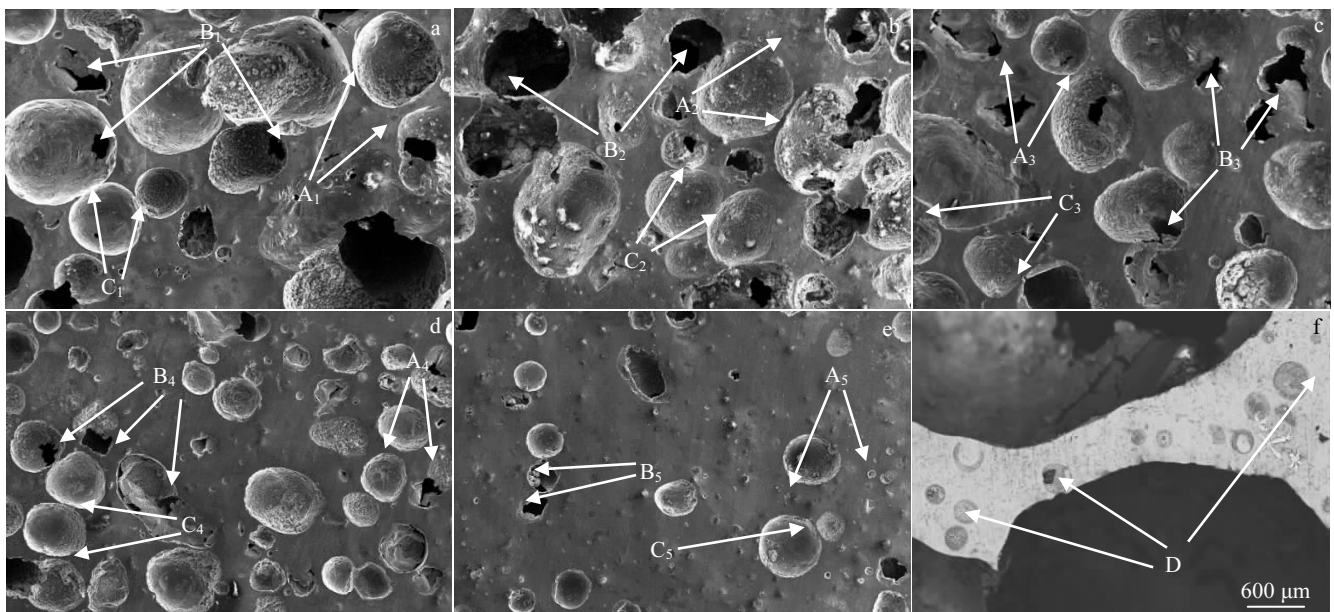


Fig.1 SEM images of cell of Mg-based foam biomaterials with different porosities: (a) $P=75.3\%$, (b) $P=72.1\%$, (c) $P=68.3\%$, (d) $P=47.1\%$, and (e) $P=38.9\%$; (f) cell edge of Mg-based foam biomaterials ($P=68.3\%$) ($A_1\sim A_5$ indicate heterogeneities, $B_1\sim B_5$ indicate fractured or missed cell walls, $C_1\sim C_5$ indicate cell-wall buckling, and D indicates HA particles)

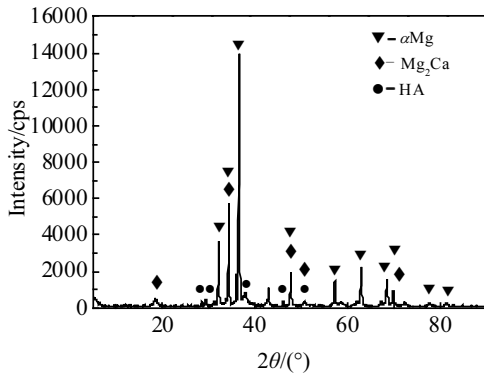


Fig.2 XRD pattern of Mg alloy matrix composites reinforced by HA

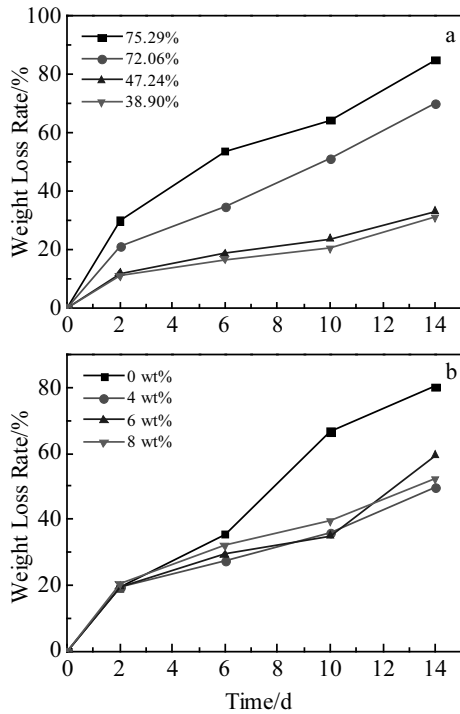


Fig.3 Change of weight loss rate of the specimens versus immersion time in the SBF media at 37±0.5 °C: (a) specimens with different total porosities and (b) specimens with different HA contents

implant should provide mechanical stability during the first two months, and then it should gradually degrade to allow invasion of cells and blood vessels to provide optimal nutrition for the regenerative tissue^[14,15,22]. Therefore, Mg-based foam biomaterials still have a high degradation rate, resulting in an early weakening of their mechanical strength. However, it is known that the degradation rate of Mg alloys in vivo is much lower than that in vitro. Witte et al^[23] have reported a 4-fold increase in the degradation rate of a Mg alloy in vitro compared to in vivo.

Fig.3b shows the variation of the weight loss rate with immersion time for specimens with different HA contents (0, 4, 6, 8, wt%) at a given porosity (~68.38%) and pore diameter (0.8~1.5 mm). When the immersion time is 2 d, the weight loss rates are 19.18%, 19.6%, 19.49% and 20.51%, corresponding to the HA content of 0 wt%, 4 wt%, 6 wt% and 8 wt%, respectively, showing a similar corrosion rate during the initial state of the four sets of specimens. After 14 d of immersion, the weight loss rates are approximately 80.38%, 49.68%, 59.46% and 52.21% when the HA content is 0 wt%, 4 wt%, 6 wt% and 8 wt%, respectively. It is clear that the weight loss rate of the specimen without HA is much larger than that of the specimen with HA. Therefore, the appropriate addition of HA particles in the specimen can extend the service time. This may be attributed to the influence of HA on the characteristics of the matrix material and the cell structure of Mg-based foam biomaterials.

Fig.4a shows the change in the open porosities of the specimens with different total porosities during the immersion period. As seen, Mg-based foam biomaterials with different total porosities have a certain number of open cells before the immersion test. This makes it possible for the SBF solution to enter the cells through the open section in the initial stage of the immersion test. Meanwhile, it can be seen that as the immersion time increases, the open porosities of the four sets of specimens increase. In the fixed immersion time, the open porosities increase with the increase in the total porosities. After 14 d of immersion, the open porosities of the specimens

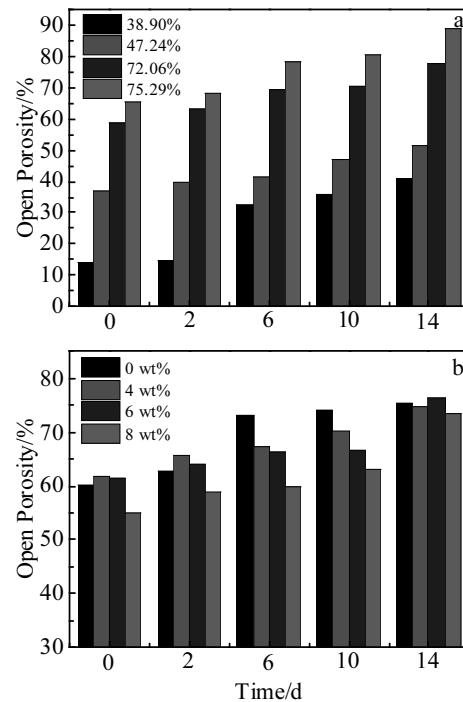


Fig.4 Change of open porosities of the specimens with total porosities (a) and HA contents (b) versus immersion time

are 40.85 %, 51.74 %, 77.69 % and 88.91 %, corresponding to the total porosities of 38.90 %, 47.24 %, 72.06 % and 75.29 %, respectively. It is observed that the open porosities are close to the total porosities of the specimens. This may be caused by the degradation of the cell walls, which makes the cells be completely interconnected and decreases the weight of the specimens. When the closed cell structure becomes interconnected, the simulated body fluid can easily enter the specimens with interconnected cells and fully circulate.

Fig.4b shows the change of open porosities of the specimens with different HA contents during the immersion period. It is shown that the open porosities increase with increasing the immersion time. Before the immersion test, the open porosities of the four sets of specimens are relatively close. The open porosity of the specimen without HA is quite close to the total porosity when the immersion time is 10 d. However, the open porosities of the specimens with HA are close to the total porosities after 14 d of immersion. It is clear that the addition of HA increases the corrosion resistance of Mg-based foam biomaterials in the simulated body fluid (SBF) media.

2.3 Electrochemical measurement

To obtain further information, the immersion tests were followed by potentiodynamic polarization measurements for these specimens. Fig.5 shows the potentiodynamic polarization curves of the four sets of specimens with different HA contents (0, 4, 6, 8, wt%) at a fixed porosity (68.38%) and pore diameter (0.8~1.5 mm) in simulated body fluid solution. The calculated values are listed in detail in Table 1. It can be seen that the corrosion potential (E_{corr} , with a saturated calomel electrode (SCE) as the reference electrode) of the specimens containing HA is higher than that of the specimen without HA. The corrosion potentials of specimens are -1.71, -1.66, -1.64 and -1.63 V when the HA content is 0 wt%, 4 wt%, 6 wt% and 8 wt%, respectively. In addition, the corrosion current density (I_{corr}) of the specimen without HA is much higher than that of the specimen with HA in the anodic polarization area. As shown in Fig.5 and Table 1, the self-

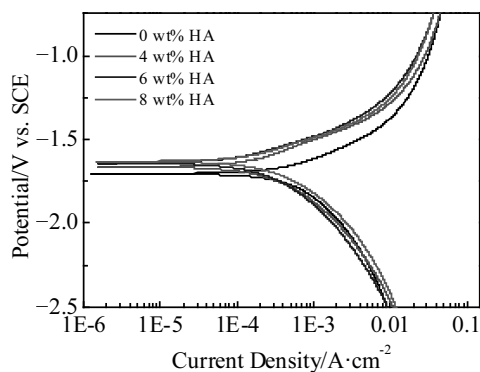


Fig.5 Potentiodynamic polarization curves of the specimens with different HA contents in the SBF media at 37±0.5 °C

Table 1 Corrosion potential (E_{corr}) and self-corrosion current density (I_{corr}) of the Mg-based foam biomaterials with different HA contents

HA content/wt%	0	4	6	8
E_{corr}/V	-1.71	-1.66	-1.64	-1.63
$I_{corr}/mA\cdot cm^{-2}$	0.68	0.23	0.23	0.21

corrosion current densities (I_{corr}) of samples with 0 wt%, 4 wt%, 6 wt% and 8 wt% HA are 0.68, 0.23, 0.23, and 0.21 mA/cm², respectively. The corrosion current densities (I_{corr}) of samples with 0 wt%, 4 wt%, 6 wt% and 8 wt% HA are 16.9, 11.9, 10.1, 8.7 mA/cm², respectively, and the corrosion potential is -1.25 V. The observations reveal that Mg-based foam biomaterial with HA possesses higher corrosion resistance than that without HA in simulated body fluid (SBF) media. This may be attributed to the effect of HA on the characteristics of the Mg alloy matrix material and the cell structure of Mg-based foam biomaterial, resulting in a higher corrosion resistance.

2.4 Morphology of the degraded samples and phase composition of the degradation products

Fig.6 shows the corrosion morphology of the Mg-based foam biomaterials with 4 wt% and 8 wt% HA after removing the degradation products. It can be seen that most of the cells are corroded into interconnected pores, while the structure of Mg-based foam biomaterials is still integrated, leading to a complex 3D interconnected porous structure of Mg-based

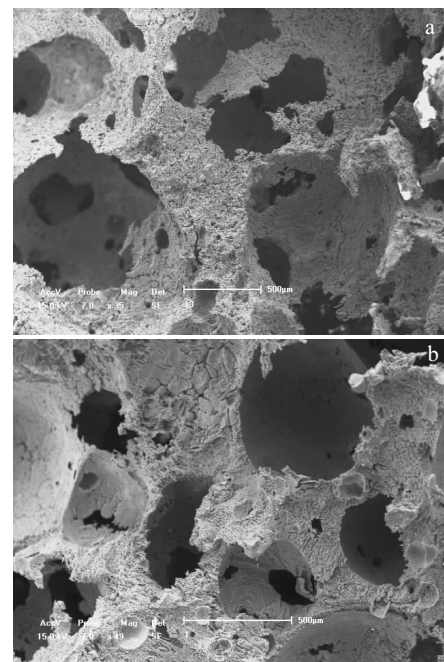


Fig.6 Corrosion morphology of the Mg-based foam biomaterials with 4 wt% (a) and 8 wt% (b) HA after immersing in SBF media for 7 d and then removing degradation products

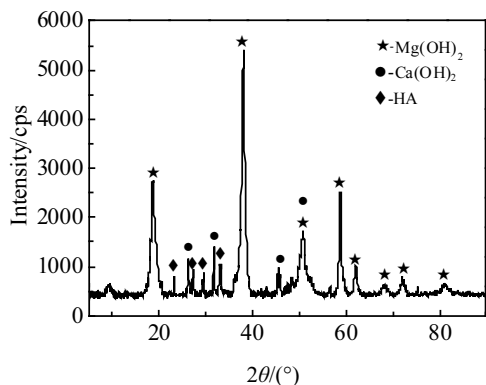


Fig.7 XRD pattern of biodegradation products

foam in the simulated body fluid (SBF) immersion test. During the bone tissue formation, the structures of the Mg-based foam biomaterials make it possible to facilitate the migration and proliferation of osteoblasts and mesenchymal cells as well as vascularization.

XRD pattern of the biodegradation products is shown in Fig.7. It is found that the biodegradation products are mainly composed of $Mg(OH)_2$, $Ca(OH)_2$ and HA. It has been reported that $Mg(OH)_2$ and $Ca(OH)_2$ do not induce toxicity to cells^[11]. Hydroxyapatite (HA) is currently used as a biomedical material and exhibits excellent biocompatibility and bioactivity due to its chemical and structural similarity to bone and tooth minerals^[10].

3 Conclusions

1) Closed-cell Mg-based foam biomaterials with total porosities of 19.81%~89.1% are produced by melt foaming process using $MgCO_3$ as a blowing agent.

2) In the immersion test, with the increase of immersion time, the weight loss rates of the specimens increase. The weight loss rate increases with the rise in total porosity of the specimen in a fixed time. This means that the higher the total porosities of the specimens, the higher the weight loss rate. Furthermore, the weight loss rate of the specimen without HA addition is much higher than that of the specimen added with HA. The weight loss rates of the specimens with different amounts of HA are similar.

3) The open porosity of the specimen increases as the immersion time increases. After 14 d of immersion, the open porosities are close to the total porosities. Meanwhile, the open porosities increase with increasing the total porosities in the fixed immersion time. The addition of HA can relatively decelerate the development of open porosity compared to the specimens without HA addition.

4) Most of the cells in the Mg-based foam biomaterials are corroded into interconnected pores, and the structure of

Mg-based foam biomaterials is still integrated. The biodegradation products are mainly composed of $Mg(OH)_2$, $Ca(OH)_2$ and HA.

5) Mg-based foam biomaterials with HA possess higher corrosion resistance than that without HA in simulated body fluid (SBF) media. The effect of HA content on the corrosion current density (I_{corr}) and corrosion potential is not significant.

References

- Geng F, Tan L, Zhang B C et al. *Journal of Materials Science & Technology*[J], 2009, 25(1): 123
- Shahini A, Yazdimamaghani M, Walker K J et al. *International Journal of Nanomedicine*[J], 2013, 9(1): 167
- Dong J, Kojima H, Uemura T et al. *Journal of Materials Research*[J], 2001, 57(2): 208
- Zhang M L, Ruan C S, Dou S H et al. *Material Letters*[J], 2013, 93: 282
- Yazdimamaghani M, Vashae D, Assefa S et al. *Journal of Biomedical Nanotechnology*[J], 2014, 10(6): 911
- Kim J K, Yaszemski M J, Lu L C. *Tissue Engineering Part C-Methods*[J], 2009, 15(4): 583
- El-Sherbiny I M, Yacoub M H. *Global Cardiology Science & Practice*[J], 2013, 38(3): 316
- Karageorgiou V, Kanplan D. *Biomaterials*[J], 2005, 26: 5474
- Salahinejad E, Hadianfard M J, Macdonald D D et al. *Plos One*[J], 2013, 8(4): 61 633
- Chen B, Yin K Y, Lu T F et al. *Journal of Materials Science & Technology*[J], 2016, 32(9): 858
- Liu Y C, Liu D B, Zhao Y et al. *Transactions of Nonferrous Metals Society of China*[J], 2015, 25(10): 3339
- Gu X N, Zhou W R, Zheng Y F et al. *Material Letters*[J], 2010, 64(17): 1871
- Yazdimamaghani M, Razavi M, Vashae D et al. *Material Letters*[J], 2014, 132: 106
- Witte F, Ulrich H, Rudert M et al. *Journal of Biomedical Materials Research Part A*[J], 2007, 81(3): 748
- Witte F, Reifenrath J, Müller P P et al. *Materials Science and Engineering Technology*[J], 2006, 37(6): 504
- Huang W Z, Luo H J, Lin H et al. *Journal of Materials Engineering and Performance*[J], 2016, 25(2): 587
- Gu X N, Zhou W R, Zheng Y F et al. *Acta Biomaterialia*[J], 2010, 6(12): 4605
- Shadanbaz S, Dias G J. *Acta Biomaterialia*[J], 2012, 8(1): 20
- Llich J Z, Kerstetter J E. *Journal of the American College of Nutrition*[J], 2000, 19(6): 715
- Li Z, Gu X, Lou S et al. *Biomaterials*[J], 2008, 29(10): 1329
- Gu X, Zheng Y, Cheng Y et al. *Biomaterials*[J], 2009, 30(4): 484
- Qiu Y S, Shahgaldi B F, Revell W J et al. *Osteoarthritis and Cartilage*[J], 2003, 11(11): 810
- Witte F, Fischer J, Nellesen J et al. *Biomaterials*[J], 2006, 27(7): 1013

骨组织工程用镁基泡沫生物材料的制备与其体外降解行为

黄闻战, 罗洪杰, 穆永亮, 徐建荣

(东北大学 先进材料制备技术教育部工程研究中心, 辽宁 沈阳 110819)

摘要: 采用熔体发泡法制备了一种镁基泡沫生物材料, 其中以镁钙合金为基体材料, 羟基磷灰石 (HA) 为增粘剂, 碳酸镁 ($MgCO_3$) 为发泡剂。对结构均匀的镁基泡沫生物材料进行测试, 研究其生物可降解行为。用腐蚀前后的孔结构、浸泡试验和电化学测试对镁基泡沫材料的生物可降解性进行表征。结果表明, 在固定时间内随着试样孔隙率的增加, 失重率不断增加; 相比于添加了 HA 的样品, 不含 HA 颗粒的样品呈现出更高的质量损失率。同时, Mg 基泡沫生物材料的总孔隙率和 HA 含量均对 Mg 基泡沫材料的开孔率有重要的影响。在相同时间内, 开孔率随试样总孔隙率的增加而增加。在模拟体液 (SBF) 介质中, 含有 HA 的 Mg 基泡沫生物材料比不添加 HA 的试样具有更高的耐腐蚀性。

关键词: 镁基泡沫材料; 生物材料; 生物降解行为; 浸泡实验; 电化学实验; 羟基磷灰石颗粒

作者简介: 黄闻战, 男, 1989 年生, 博士生, 东北大学冶金学院, 辽宁 沈阳 110819, 电话: 024-83686462, E-mail: 1252805266@qq.com